Arabian Journal of Geosciences (2022) 15: 838
https://doi.org/10.1007/s12517-022-10140-3

ORIGINAL PAPER

Evaluating statistical and combine method to predict stand above-ground biomass using remotely sensed data

Sinan Bulut[1] · Fatih Sivrikaya[2] · Alkan Günlü[1]

Received: 31 December 2021 / Accepted: 13 April 2022 / Published online: 23 April 2022

Abstract
Above-ground biomass (AGB) is a key parameter as indicator of forest carbon content and ecosystem productivity. Producing highly predictive models and spatial distribution of AGB stocks support the development of forest management plans. In this research, AGB was modeled using multiple linear regression (MLR) analysis and regression kriging (RK) techniques. Reflectance and vegetation indices data derived from the Sentinel-2 satellite images were used as an auxiliary variable. The highest correlation coefficients between the AGB and remote sensing data were obtained in broadleaf stands. These values were 0.743 and 0.869 for reflectance values of B8 band and PSSR vegetation index values, respectively. The AGB contents of coniferous, broadleaf, and mixed stands were modeled separately with MLR method. Then, RK method performed with combining MLR and ordinary kriging methods. The R^2 values of MLR method were lower than 0.80. Ordinary kriging method was applied to MLR residuals, and it was determined that the highest spatial dependence was in coniferous stands (spatial correlation index = 57–60). The highest explained variance proportions for RK method were 0.88, 0.84, and 0.83 in coniferous, broadleaf, and mixed stands, respectively. Overall, the accuracy of MLR method was not sufficient for AGB estimation, but the combination of kriging helped to take advantage in terms of improving the accuracy of AGB predictions. To increase the accuracy of the AGB model, it is thought that it would be beneficial to diversify the remote sensing data and to combine the kriging method with different techniques.

Keywords Above-ground biomass · Sentinel-2 · Semivariogram analysis · Regression kriging

Introduction

Estimating and monitoring stand above-ground biomass (AGB) provide crucial information for forest ecosystem productivity, carbon sequestration, decision-making process, nutrient allocation, sustainable forest management strategies, and functional and structural attributes of forest ecosystems in various environmental conditions (Ali et al. 2012, 2019; Hall et al. 2006). According to Kyoto agreement and international negotiations, forest management plans require biomass and carbon storage data and Turkey has to declare contribution of forest to the carbon cycle.

Quantifying the amount of carbon sequestration in forests requires spatially detailed forest biomass and changes in forest carbon stocks. Therefore, forest biomass should be estimated accurately to evaluate the role of forests in the global carbon cycle (Ali et al. 2012; Ali and Abbas 2013; Tsui et al. 2013; Abbas et al. 2020; Bhat et al. 2021). The AGB can be measured or predicted both directly and indirectly. Prediction of the AGB with direct method, which known as harvest method, is more accurate method for calculating biomass, but needs more effort due to the destructiveness, time, cost, and labor, especially for large areas. The indirect methods involve the prediction based on allometric equations or remote sensing (Goetz et al. 2009; Englhart et al. 2011; Deb et al. 2017; Motlagh et al. 2018; Abbas et al. 2020).

Responsible Editor: Haroun Chenchouni

Sinan Bulut
sbulut@karatekin.edu.tr

Fatih Sivrikaya
fsivrikaya@kastamonu.edu.tr

Alkan Günlü
alkangunlu18@gmail.com

[1] Department of Forest Management, Faculty of Forestry, Çankırı Karatekin University, 18200 Çankırı, Türkiye

[2] Department of Forest Management, Faculty of Forestry, Kastamonu University, 37150 Kastamonu, Türkiye

Remote sensing is an appropriate method for predicting forest biomass and has been the most commonly used approach to estimate AGB due to the relative ease, quick, and low cost of acquiring remotely sensed data over wide and often nearly inaccessible forest areas (Goetz et al. 2009; Tian et al. 2012; Motlagh et al. 2018; Abbas et al. 2020). The biomass values are not directly estimated using remote sensing data, but it is computed using statistical relationships between the spectral features, which primarily consist of different vegetation indices, and AGB data collected from sample plots (Motlagh et al. 2018; Abbas et al. 2020; Ronoud et al. 2021). In recent years, several studies have demonstrated that satellite spectral information (band ratios, band transformations, spectral band) and vegetation indices combined with field measurements has a good relationship with AGB (Lu 2006; Viana et al. 2012).

Satellite image such as Sentinel-2, intermediate spatial resolution, is a practical product and commonly used due to the relevance of the spectral bands, and the suitable spatial resolution. Sentinel-2 multispectral image files with a ground resolution of up to 10 m are now freely accessible. Researchers frequently utilize data to derive remote sensing parameters, and the revisit time is 3 days. Sentinel-2 data have three vegetation red edge, two infrareds, visible, and near infrared bands. The Sentinel-2 satellite was launched for the first time on June 23, 2015; data are influenced by cloud cover, and no previous Sentinel-2 datasets are available (Chen et al. 2019a; Abbas et al. 2020; Wang and Jiao 2020). Clerici et al. (2016) used linear models and vegetation indices to estimate AGB and carbon in Colombian forests using Pleiades-1A and GeoEye-1 satellites. In Turkey, Günlü et al. (2014) used multiple regression models to investigate the relationship between ABG and vegetation indices using spectral bands from the Landsat TM satellite, and concluded that vegetation indices have better performance in prediction of the AGB compared to spectral bands. Kumar et al. (2016) found that using a combination of spectral indices from Landsat-8 satellite data and ALOS-2 radar to estimate biomass had better results than using these indices individually.

Qualitative visual analysis reveals spatial enhancements as well as spectral information retention, allowing super-resolved Sentinel-2 images to be utilized in research that need extremely high spatial resolution (Romero et al. 2020). Various relationships have been developed between vegetation indices and AGB using Sentinel-2. Pandit et al. 2018 developed a novel AGB estimate approach and showed how medium-resolution Sentinel-2 Multi-Spectral Instrument (MSI) data may be used instead of hyperspectral data in inaccessible areas. The model using spectral information and vegetation indices provided better AGB estimates. To estimate AGB, optical images from Sentinel-2 were utilized as auxiliary information. The most relevant factors among optical data for predicting AGB were indices using the NIR spectrum (B8 and B8A) and red edge bands, and the approach used in this study may offer reliable and cost-effective estimations of AGB (Navarro et al. 2019). The Sentinel series data have been used in a variety of vegetation studies (Sibanda et al. 2015; Laurin et al. 2016; Mura et al. 2018). The use of Sentinel data for forest AGB mapping, on the other hand, requires more investigation (Chen et al. 2019a).

Generally, the AGB can be estimated from satellite images by using various techniques such as geostatistics, multiple linear regression (MLR), and k-nearest-neighbor classification (Zheng et al. 2004; Labrecque et al. 2006; Ji et al. 2012). Geostatistics were developed to analyze and describe the variation in both natural and man-made occurrences (Cressie 1993; Viana et al. 2012). Geostatistics comprise a set of techniques for estimating uncertainty and relies upon the interpretation of reflectance as a function of spatial position. There are several geostatistical methods that use ancillary data to improve the prediction accuracy of the variables (Castillo-Santiago et al. 2013; Hengl et al. 2007; Goovaerts 2000). These are ordinary kriging, co-kriging, and kriging with external drift. Combine methods such as geographically weighted regression-kriging, regression kriging (RK), support vector machine-kriging, and random forest-kriging have been widely used techniques for modeling environmental variables using remotely sensed data (Benitez et al. 2016; Su et al. 2020; Chen et al. 2019b, 2020). Several approaches for predicting stand biomass using satellite image data have been developed in the world, but studies using geostatistics for estimating forest biomass in Turkey are limited.

The study is a comparative analysis between MLR and RK methods using reflectance and vegetation indices values obtained from Sentinel-2 satellite image for modeling the AGB of forest types in the northern Turkey. The objectives were (1) to identify satellite-derived reflectance values and vegetation indices that are better associated with AGB, (2) to quantify spatial patterns of the AGB predictions derived from MLR and RK methods, and (3) to determine whether RK method improves the estimates of AGB pools over MLR method.

Material and methods

Study area

The study area is located in the Ilgaz Forest Enterprise, which is under control of Ankara Regional Directorate of Forestry in the north region of Turkey (Fig. 1). The study area is spanning from 498,234 to 572,705 east longitudes and from 4,496,441 to 4,548,108 north latitudes in WGS 1984 datum zone 36th according to UTM

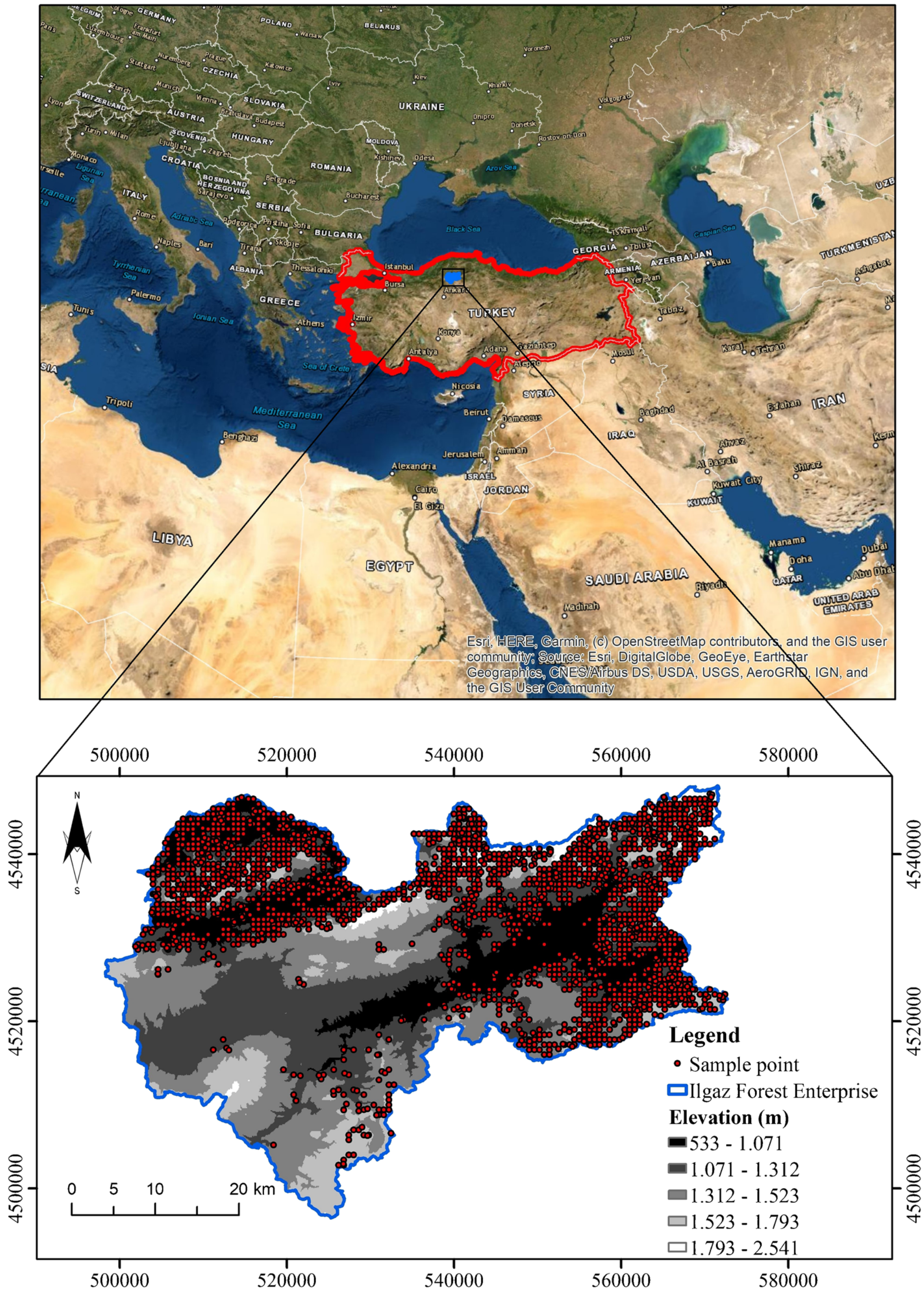

Fig. 1 The location of the study area, including the elevation map and sample point

coordinate system. The study area is 205169.6 ha and, productive forest cover nearly 20.0% of the study area (41,527.2 ha). Total forest area is 74847.91 ha. The forest areas in the region are natural and the even-aged forests are 71,916.30 ha, and the uneven-aged forests are 2931.61 ha. The areas of coniferous, broadleaf, and mixed stands are 45,746.88, 20,559.12, and 8541.91 ha, respectively. The majority of forest areas consist of coniferous forests (61%). The elevation ranges from 533 to 2541 m above sea level with an average slope of 20%. The primary tree species of the vegetation are *Abies* sp. (Fir), *Pinus sylvestris* (Scots pine), *Pinus nigra* (Black pine), *Quercus* sp. (Oak), and *Fagus* sp. (Beech), which might be standing as either pure or mixed stand types. The mean annual temperature recorded so far in the study area is 10.6 °C and mean annual precipitation is 418.6 mm (Anonymous 2018).

Field data and biomass estimation

The field data were based on ground measurements obtained from forest inventory. The forest inventory was made with the systematic sampling (300 × 300 m) method in 2018 by the General Directorate of Forestry of Turkey for the purpose of preparing forest management plans. Forest management plans and forest cover type map were used in this study. The growing stock volume of each stand type was obtained from the forest management plans, and the growing stock volume map was created by using Geographic Information Systems (GIS). Biomass expansion factor (BEF) was used to estimate biomass, and reference map was created for stand AGB. BEF converts growing stock volume to above-ground biomass (AGB) to account for components of tree such as branches and leaves (Teobaldelli et al. 2009). The most important data source for estimating forest biomass in the BEF method is growing stock inventory data since it is easily measured and often available in national forest database (Schroeder et al. 1997; Hu and Wang 2008). The AGB was estimated by multiplying growing stock obtained from forest inventory data, BEF, and wood density (oven-dry weight coefficient).

$$AGB = GS \times BEF \times WD \tag{1}$$

where AGB: above-ground biomass (ton/ha), GS: growing stock (standing timber volume, m^3/hectare), BEF: biomass expansion factor, WD: wood density. AGB was calculated using the BEF coefficients (1.212 for coniferous and 1.310 for broadleaf tree species) and WD (0.446 for coniferous and 0.541 for broadleaf tree species) coefficients developed by Tolunay (2011). Thus, AGB of each stand type was calculated using related coefficients.

Image processing

Sentinel-2 satellite image (June 21, 2018), which was downloaded free of charge from the USGS Earth Explorer data portal, was used in this study. The ten bands (bands 2, 3, 4, 5, 6, 7, 8, 8A, 11, and 12) of Sentinel-2 with 10–20 m spatial resolutions were used. The atmospheric correction was made to prepare the image ready for analysis. The ten bands of the Sentinel-2 satellite image were used and the reflectance values of these bands were calculated separately by using the QGIS 3.8.1 software. The average reflectance values of all pixels in each forest cover type maps were calculated using the zonal statistics function in the ArcGIS 10.6.1 software. Thus, the average reflectance values of each stand type were calculated. In addition, 24 different vegetation indices were calculated based on average reflectance values (Table 1). A total of 2185 sample points were placed using GIS, one for each stand type. The AGB and reflectance and vegetation indices were calculated in all sample points. The AGB modeling was performed separately with reflectance and vegetation indices for coniferous, broadleaf, and mixed stands.

Modeling process and the validation of AGB map results

The AGB and remote sensing data of 2185 points from the field area were prepared for modeling. Data from three forest types were used for performing multiple linear regression (MLR) method. Then, data sets were separated by 80–20% as model and test data to validation of the AGB map results obtained from regression kriging (RK) method. The data numbers allocated for the model-test data were determined as 1154–289 for coniferous stands, 403–101 for broadleaf stands, and 190–48 for mixed stands. The implementation of RK method was carried out in two stages. The RK method was performed using the model data sets. The validation process was carried out by comparing the RK predictions made in the test points with the observation data.

Multiple linear regression

The MLR has been used to define the relationships between AGB and satellite data. Parameters that are difficult to measure are estimated by modeling with remote sensing data (reflectance, vegetation indices and texture values). We researched on the forecastable of AGB using the MLR method based on Sentinel-2 data. The variables obtained from Sentinel-2 were tested at 0.05 significance level using the stepwise selection technique in the SPSS® software.

$$f(AGB) = b_0 + b_1x_1 + b_2x_2 + \cdots + b_ix_i \tag{2}$$

where AGB is the target variable to be predicted, a_0 is a constant coefficient, and $b_{1....i}$ and $x_{1....i}$ are the regression coefficients and values of auxiliary variables.

Regression kriging

The RK method is a combine method that involves either a MLR model between the dependent and independent variables, the MLR residuals, and performing kriging to MLR residuals (Odeh et al. 1994; 1995). The sample plots in the same field are dependent and spatially correlated. For this reason, it is important to consider spatial autocorrelation in datasets to increase model accuracy when fitting a model. The MLR method does not consider the spatial autocorrelation in data. The RK method, on the other hand, can improve the accuracy of the predictions as it takes into account the spatial autocorrelation of residuals in the MLR model.

Table 1 Vegetation indices derived from Sentinel-2 satellite image

Vegetation indices	Formula	References	Vegetation indices	Formula	References
NDVI (normalized difference vegetation index)	(B08 − B04) / (B08 + B04)	Rouse et al. (1974)	GLI (green leaf index)	(2.0 × B03 − B04 − B02) / (2.0 × B03 + B04 + B02)	Louhaichi et al. (2001)
GNDVI (green normalized difference vegetation index)	(B08 − B03) / (B08 + B03)	Gitelson et al. (1996)	CHL-R-E (Chlorophyll Red-Edge)	(B07 / B05) − 1	Gitelson et al. (2005)
BNDVI (blue-normalized difference vegetation index)	(B08 − B02) / (B08 + B02)	Wang et al. (2007)	CCCI (Canopy Chlorophyll Content Index)	((B08 − B05) / (B08 + B05)) / ((B08 − B04) / (B08 + B04))	Fitzgerald et al. (2010)
MNDVI (modified normalized difference vegetation index)	(B08 − B12) / (B08 + B12)	Jurgens (1997)	CHLG (Chlorophyll Green)	(B07 / B03) − 1	Gitelson et al. (2003)
GBNDVI (green–blue NDVI)	(B08 − (B03 + B02)) / (B08 + (B03 + B02))	Wang et al. (2007)	CLR Edge (Chlorophyll IndexRedEdge)	(B08 / B05) − 1.0	Gitelson et al. (2003)
GRNDVI (green–red NDVI)	(B08 − (B03 + B04)) / (B08 + (B03 + B04))	Gitelson and Merzlyak (1996)	CVI (Chlorophyll vegetation index)	B08 × (B04 / B03^2)	Vincini et al. (2007)
NDWI (normalized difference water index)	(B08 − B11) / (B08 + B11)	McFeeters (1996)	LCI (Leaf Chlorophyll Index)	(B08 − B05) / (B08 + B04)	Thenkabail et al. (1999)
WDVI (weighted difference vegetation index)	(B08 − a × B04); a = 0.460	Clevers (1989)	MCARI (Modified Chlorophyll Absorption in Reflectance Index)	((B05 − B04) − 0,2x(B06 − B03)) x(B05/B04)	Daughtry et al. (2000)
EVI (enhanced vegetation index)	2.5 × (B08 − B04) / ((B08 + 6.0 × B04 − 7.5 × B02) + 1.0)	Liu and Huete (1995)	MCARI1 (Modified Chlorophyll Absorption in Reflectance Index)	((B05 − B04) − 0.2 × (B05 − B03)) × (B05 / B04)	Haboudane et al. (2004)
EVI2 (enhanced vegetation index 2)	2.4 × (B08 − B04) / (B08 + B04 + 1.0)	Jiang et al. (2008)	PSSR (Pigment Specific Simple Ratio)	(B08 / B04)	Blackburn (1998)
SAVI (soil adjusted vegetation index)	(B08 − B04) / (B08 + B04 + L) × (1.0 + L); L = 0.428	Huete (1988)	MSI (Moisture Stress Index)	(B11 / B08)	Hunt and Rock (1989)
NLI (nonlinear vegetation index)	((B08^2) – (B04)) / ((B08^2) + (B04))	Goel and Qin (1994)	GVMI (Global Vegetation Moisture Index)	((B08 + 0.1) − (B12 + 0.02)) / ((B08 + 0.1) + (B12 + 0.02))	Ceccato et al. (2002)

The implementation of the RK method was carried out in 3 stages. Firstly, MLR analysis was performed to find significant parameters among the independent variables to be used in the MLR model. Then, the ordinary kriging method was applied to the residuals from MLR model estimations using the ArcGIS 10.6.1 software. In the last stage, the RK predictions were obtained by adding kriged residuals to MLR estimates (Odeh et al. 1995) (Fig. 2). In addition, the spatial correlation index (SCI) was calculated (Cambardella et al. 1994). Cambardella et al. (1994) suggested that variables with a nugget ratio < 25% are accepted to be strongly, between 25 and 75% moderately, and > 75% weakly spatially dependent.

$$SCI = \left(\frac{\text{Nugget}}{\text{Sill}}\right) \times 100 \quad (3)$$

$$\hat{Z} = \varphi_0 + \sum_{i=1}^{n} \varphi_i x_i(s) + \sum_{j=1}^{m} \lambda_i \varepsilon(s_i) \quad (4)$$

where φ_0 and φ_i are the MLR predictions, $x_i(s)$ is an auxiliary variable that accounts for target variable variation, n is the number of observations, λ_i is kriging weight, and $\varepsilon(s_i)$ is the kriged residual at field location (Fig. 2).

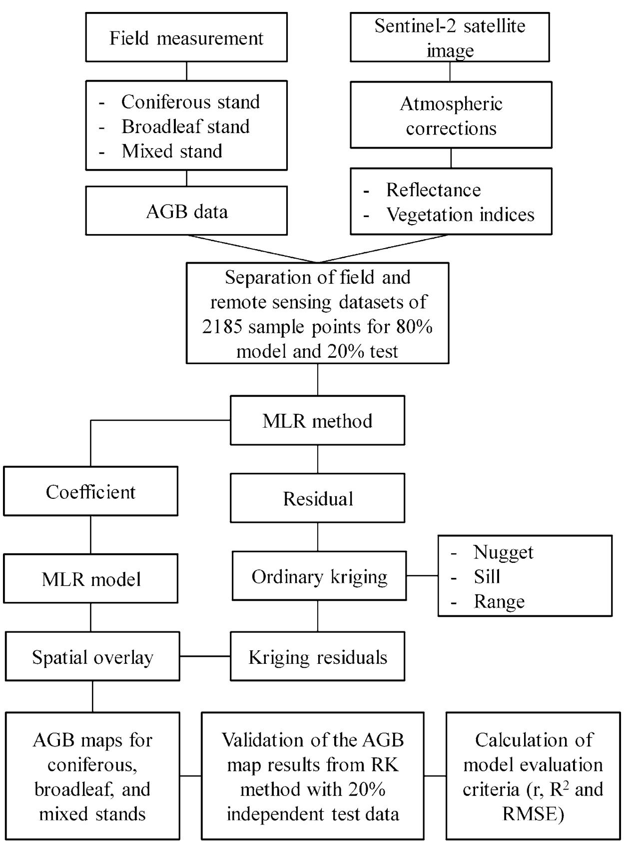

Fig. 2 Framework of the system design to predicting stand biomass using MLR and RK method for coniferous, broadleaf, and mixed stands

Results

The mean AGB of the total forest areas was 76.70 (ton/ha) in the study area (Table 2). Minimum AGB values were between 1.42 and 4.36 (ton/ha) and were close for three forest types. Among forest types, the highest mean AGB belonged to coniferous stands (106.95 ton/ha). AGB contents of broadleaf and mixed stands were lower than coniferous stands, and mixed stands had the lowest mean AGB (19.31 ton/ha).

Significant correlations were found between AGB-reflectance and AGB-vegetation indices. The highest correlations among the three forest types were found for broadleaf stands. The highest correlation coefficients between the AGB and reflectance values were obtained with B11 ($r = -0.677$), B8 ($r = 0.743$), and B2 ($r = -0.607$) bands for coniferous, broadleaf, and mixed stands, respectively (Table 3). The highest correlation coefficients among the vegetation indices were found with CHL-R-E in coniferous ($r = 0.690$) and mixed stands ($r = 0.769$), and PSSR in broadleaf stands ($r = 0.869$) (Table 4). The lowest correlation coefficients between AGB and reflectance values were obtained in the B6 and B8A bands. Negative correlations were found between the AGB content of coniferous stands and the reflectance values of all bands. The lowest correlation relationship level between AGB and vegetation indices was determined for coniferous stands with MCARI1 index ($r = -0.005$).

The AGB was estimated for coniferous, broadleaf, and mixed stands using reflectance values and vegetation indices according to MLR method (Tables 5, 6). The same explanatory variables were B6, B7, B8, and B11 in modeling coniferous and broadleaf stands with reflectance values. In three forest types, reflectance values of band 6 were included as explanatory variable in the MLR models. In MLR models performed with vegetation indices, six similar independent variables (CHL-R-E, PSSR, CHLG, LCI, EVI, and MCARI) were determined for coniferous and mixed stands. PSSR

Table 2 Descriptive statistics for AGB (ton/ha) of the coniferous, broadleaf, mixed stands, and total forest area

Forest type	Count	Min	Max	Mean	Std. D
Coniferous stand	1443	1.42	405.02	106.95	85.84
Broadleaf stand	504	1.42	207.10	20.83	38.68
Mixed stand	238	4.36	163.80	19.31	32.43
Total forest area	2185	1.42	405.02	76.70	83.50

Table 3 Pearson's correlation coefficients between AGB and reflectance values

Forest type	Variable	Reflectance									
		B2	B3	B4	B5	B6	B7	B8	B8A	B11	B12
Coniferous stand	AGB (ton/ha)	−0.674[b]	−0.676[b]	−0.644[b]	−0.674[b]	−0.526[b]	−0.433[b]	−0.442[b]	−0.442[b]	−0.677[b]	−0.656[b]
Broadleaf stand		−0.645[b]	−0.618[b]	−0.656[b]	−0.594[b]	0.668[b]	0.741[b]	0.743[b]	0.731[b]	−0.442[b]	−0.594[b]
Mixed stand		−0.607[b]	−0.598[b]	−0.569[b]	−0.576[b]	−0.022[a]	0.122[a]	0.118[a]	0.089[a]	−0.540[b]	−0.552[b]

[a]Correlation is not significant

[b]Correlation is significant at the 0.01 level

Table 4 Pearson's correlation coefficients between AGB and vegetation indices values

Forest type	Variable	Vegetation indices							
		NDVI	GNDVI	BNDVI	MNDVI	GBNDVI	GRNDVI	MCARI	MCARI1
Coniferous stand	AGB (ton/ha)	0.603[b]	0.620[b]	0.554[b]	0.653[b]	0.598[b]	0.618[b]	−0.360[b]	−0.005[a]
Broadleaf stand		0.744[b]	0.749[b]	0.733[b]	0.738[b]	0.763[b]	0.770[b]	0.601[b]	0.795[b]
Mixed stand		0.613[b]	0.638[b]	0.605[b]	0.634[b]	0.642[b]	0.647[b]	0.049[a]	0.435[b]
		CHL-R-E	CCCI	CHLG	CLR Edge	CVI	LCI	SAVI	EVI
Coniferous stand	AGB (ton/ha)	0.690[b]	0.594[b]	0.645[b]	0.683[b]	0.627[b]	0.648[b]	0.107[b]	0.025[a]
Broadleaf stand		0.848[b]	0.266[b]	0.849[b]	0.848[b]	0.770[b]	0.762[b]	0.792[b]	0.802[b]
Mixed stand		0.769[b]	0.558[b]	0.746[b]	0.762[b]	0.704[b]	0.652[b]	0.491[b]	0.464[b]
		EVI2	PSSR	NDWI	MSI	WDVI	GVMI	NLI	GLI
Coniferous stand	AGB (ton/ha)	−0.004[a]	0.598[b]	0.688[b]	−0.673[b]	−0.314[b]	0.664[b]	0.351[b]	0.380[b]
Broadleaf stand		0.796[b]	0.869[b]	0.732[b]	−0.686[b]	0.785[b]	0.641[b]	0.812[b]	0.786[b]
Mixed stand		0.449[b]	0.734[b]	0.685[b]	−0.632[b]	0.267[b]	0.579[b]	0.603[b]	0.582[b]

[a]Correlation is not significant

[b]Correlation is significant at the 0.01 level

Table 5 MLR model to estimate AGB using reflectance values for coniferous, broadleaf, and mixed stands

Coniferous stand				Broadleaf stand			
Parameter	Coefficient	*t*	*p*	Parameter	Coefficient	*t*	*p*
(Constant)	271.278	15.219	0.000	(Constant)	21.303	2.186	0.029
B3	9951.816	4.218	0.000	B7	6856.775	9.639	0.000
B4	4201.580	3.278	0.001	B6	−5151.770	−12.228	0.000
B11	−1049.775	−2.246	0.025	B8A	−4637.706	−8.377	0.000
B7	10,116.546	9.361	0.000	B11	384.845	6.381	0.000
B6	−8795.343	−6.329	0.000	B8	2319.108	3.982	0.000
B12	1659.272	2.206	0.028	Mixed stand			
B8	−2836.645	−3.860	0.000	Parameter	Coefficient	*t*	*p*
B2	−11,531.188	−5.548	0.000	(Constant)	90.809	4.758	0.000
B5	−6186.246	−4.854	0.000	B2	−6299.740	−5.761	0.000
				B4	10,513.624	10.880	0.000
				B5	−9057.291	−10.269	0.000
				B6	1757.224	9.572	0.000

indices for three forest types was statistically significant to estimate AGB and included in the model ($p < 0.05$).

Semivariance analysis was conducted before interpolation the AGB of coniferous, broadleaf, and mixed stands. Semivariogram graphics of the AGB residuals were shown in Fig. 3. Semivariogram models were chosen according to the lowest error. The results indicated that the smallest error was mostly obtained in the exponential model for the reflectance and vegetation indices in forest types. The spherical model was used only in mixed stands with

Table 6 MLR model to estimate AGB using vegetation indices values for coniferous, broadleaf, and mixed stands

Coniferous stand				Broadleaf stand			
Parameter	Coefficient	*t*	*p*	Parameter	Coefficient	*t*	*p*
(Constant)	174.568	6.418	0.000	(Constant)	−18.933	−11.994	0.000
MCARI	−6189.443	−3.838	0.000	PSSR	14.322	18.238	0.000
CHLG	106.785	12.021	0.000	GRNDVI	−92.060	−6.823	0.000
PSSR	−97.176	−10.515	0.000	Mixed stand			
GLI	1384.576	7.841	0.000	Parameter	Coefficient	*t*	*p*
CHL-R-E	114.411	6.635	0.000	(Constant)	123.917	6.030	0.000
LCI	−275.096	−3.527	0.000	CHL-R-E	135.290	6.061	0.000
EVI	−338.750	−3.109	0.002	PSSR	−26.629	−5.332	0.000
				CHLG	35.812	3.798	0.000
				LCI	−573.644	−6.454	0.000
				EVI	−330.443	−2.884	0.005
				MCARI	3509.070	2.075	0.040

vegetation indices due to obtaining the lowest error. Semivariogram parameters such as nugget, sill, and range of the selected semivariogram models were illustrated in Table 7. The SCI calculated as the percent nugget effect was calculated for each interpolation in forest types. It was determined that the highest spatial dependence among forest species was in coniferous stands ($SCI\% = 57$, 60). Spatial dependence was found to be low in broadleaf forests ($SCI\% = 89$, 91).

The RK predictions were obtained by adding kriged residuals to MLR estimation values. As a result of this process, success performance criteria of MLR and RK estimates were calculated for coniferous, broadleaf, and mixed stands (Tables 8, 9). As a predictor variable, the highest success in the MLR and RK methods belong to the vegetation indices values. The vegetation indices provided a better model explanatory power for all stands and methods. The best success was obtained by performed the RK method with the vegetation indices in coniferous stands ($R^2 = 0.88$). The lowest success was obtained by using the MLR method with reflectance data in coniferous stands ($R^2 = 0.64$). The lowest and highest success in coniferous stands showed that the improvement in the estimation of AGB occurred mostly in these stands.

The AGB mapping results from RK method were validated based on independent datasets. The model and test performance of the AGB based on vegetation indices were both compatible and the highest (Table 9). The most successful results for model ($R^2 = 0.84$) and test ($R^2 = 0.72$) were obtained in broadleaf stands. The lowest error was found in mixed stands (model $RMSE = 15.619$, test $RMSE = 19.759$). The lowest success was in coniferous stands for the AGB content based on reflectance values. The AGB prediction based on the vegetation indices in coniferous stands had the highest model ($R^2 = 0.88$) and the lowest test ($R^2 = 0.69$) success.

The spatial distribution of the AGB of the coniferous, broadleaf, and mixed stands was estimated using the RK method, and the surface map of the AGB was created by combining AGB maps of the forest types (Fig. 4). According to the AGB map produced by the RK method, the AGB is higher in the north-eastern part of the study area. While the AGB was in the range of 0–180 (ton/ha) in other regions, it was determined in the range of 180–450 (ton/ha) in the north-eastern part. Areas where biomass is high are mostly composed of uneven-aged pure Fir and Fir-Scotch pine mixed stands. In addition, there were old and fully closed stands of black pine in the same region. It was determined that the reference map (Fig. 4, b) and the RK prediction maps (Fig. 4, c–d) were similar in terms of the spatial distribution of the AGB. In the regions with high AGB in the reference map, the RK method made lower estimates.

Discussion

The AGB of the coniferous, broadleaf, and mixed stands was calculated. The AGB of coniferous stands had a higher data range from 2.16 to 405.02 ton/ha, and therefore, coniferous stands were more heterogeneous than other forest types in terms of development. The AGB levels of broadleaf and mixed stands were lower than coniferous stands (Table 2). When the stand structures in the area were examined, coniferous forests contained more growing stock volume. Coniferous stands were more mature, and AGB levels were higher (Anonymous 2018).

Six independent variables (CHL-R-E, PSSR, CHLG, LCI, EVI, and MCARI) in MLR models were determined for coniferous and mixed stands in Hyrcanian forests of Iran. PSSR indices for three forest types was statistically significant to estimate AGB and included in the model ($p < 0.05$). The highest relationship for predicting AGB was found to be

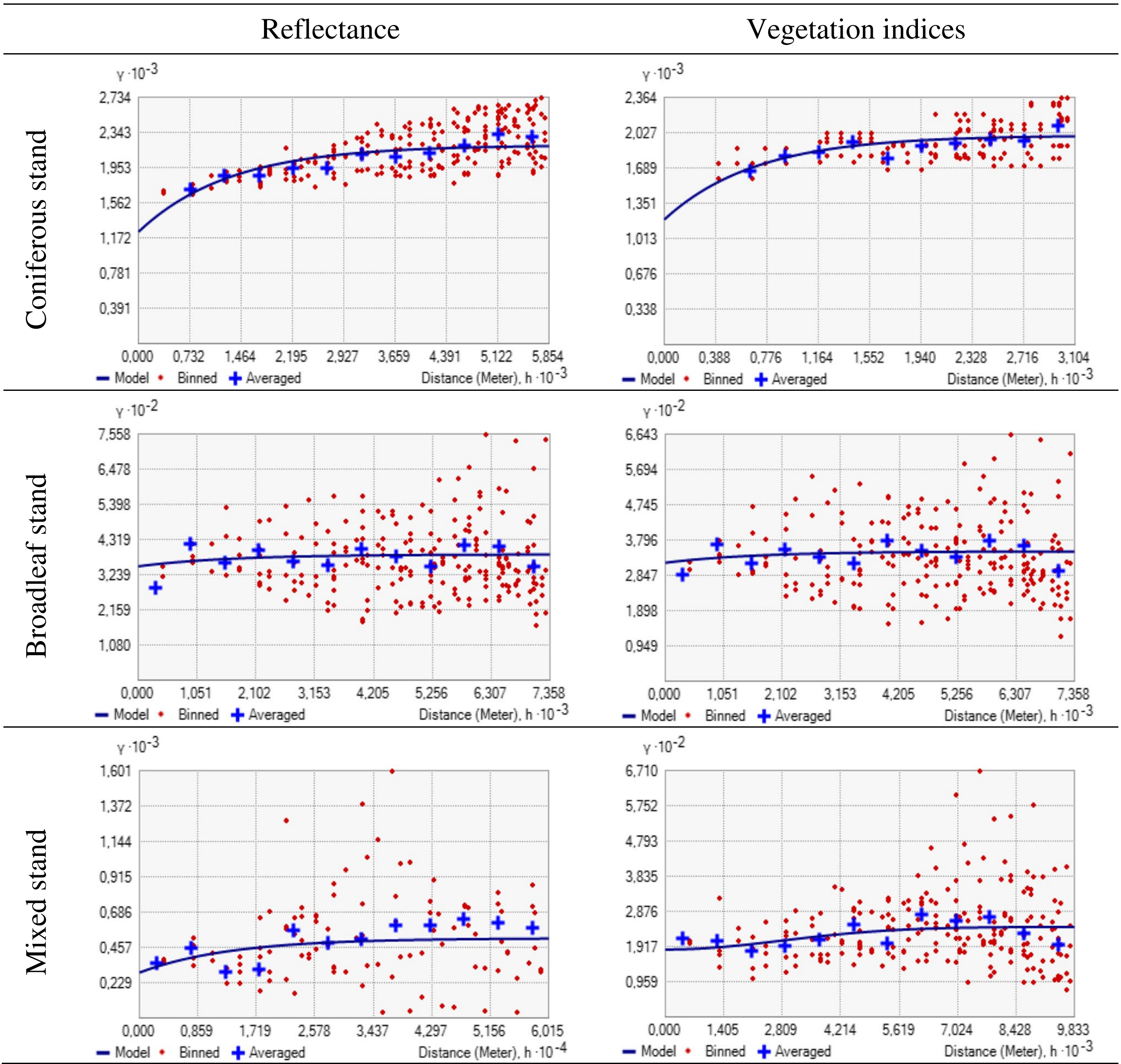

Fig. 3 Experimental semivariograms of coniferous, broadleaf, and mixed stands for AGB based on reflectance and vegetation indices data

Table 7 Semivariogram parameters of fitted models for AGB of the forest types

Forest type	Satellite data	Model	Nugget	Sill	Range	*SCI%*
Coniferous stand	Reflectance	Exponential	1239.9	2195.2	3902.8	57
	Vegetation indices	Exponential	1195.5	1986.4	2069.3	60
Broadleaf stand	Reflectance	Exponential	349.8	394.7	4905.3	89
	Vegetation indices	Exponential	318.8	350.7	4715.6	91
Mixed stand	Reflectance	Exponential	294.8	482.5	4010.2	61
	Vegetation indices	Spherical	183.9	251.7	6836.7	73

Table 8 Performance criteria of the MLR method by correlation coefficient (r), coefficient of determination (R^2), and root mean squared error (*RMSE*)

Forest type	Performance criteria	Reflectance	Vegetation indices
Coniferous stand	R^2	0.64	0.66
	r	0.80	0.81
	RMSE	48.896	47.152
Broadleaf stand	R^2	0.74	0.78
	r	0.86	0.88
	RMSE	19.437	17.926
Mixed stand	R^2	0.66	0.77
	r	0.81	0.88
	RMSE	20.983	17.123

Table 9 Validation of the AGB predictions obtained from the RK method by correlation coefficient (r), coefficient of determination (R^2), and root mean squared error (*RMSE*)

Forest type	Performance criteria	Reflectance		Vegetation indices	
		Model	Test	Model	Test
Coniferous stand	R^2	0.85	0.68	0.88	0.69
	r	0.92	0.83	0.94	0.83
	RMSE	32.412	51.275	28.105	49.729
Broadleaf stand	R^2	0.82	0.71	0.84	0.72
	r	0.91	0.84	0.92	0.85
	RMSE	17.594	23.404	16.090	21.952
Mixed stand	R^2	0.80	0.69	0.83	0.72
	r	0.89	0.83	0.91	0.85
	RMSE	18.029	21.606	15.619	19.759

NDVI, followed by RVI. RVI had a reverse relationship with the AGB (Motlagh et al. 2018). Kumar et al. (2016) reported that EVI, SAVI, and RVI vegetation indices showed a higher relationship with AGB compared to NDVI in Surat Thani Province, Thailand.

Experimental semivariogram analysis was conducted. Mostly, the exponential variogram model was better fitted. The semivariogram model parameters were obtained for interpreting spatial relationships. According to the SCI data, coniferous stands had the highest level of spatial dependence. In terms of the classification, the spatial dependence of coniferous and mixed stands was moderately. Weakly spatial dependency was found in broadleaf stands. Lack of strongly spatial dependence indicates that the variability at short distance is high and there is a weak autocorrelation in the data. The nugget value was high in our study area, suggesting small-scale variabilities, in other words, a weak spatial autocorrelation in study data. Weak spatial dependency is due to anthropogenic effects (Behera and Shukla 2015). These effects are measurement errors or spatial variation at distances smaller than the sampling interval (Li et al. 2020). The study area consists of intensively managed forests. Applied silvicultural treatments in stands effect forest structure and this situation also increases the variation of the forest structure depending on the distance. The fact that the sampling distance does not reflect this variability may causes the spatial dependence to be obtained weakly.

The AGB was predicted using MLR and RK method with reflectance and vegetation indices values as auxiliary variable. The RMSE values for coniferous stands (*RMSE* = 28.105–48.896) were higher than that for broadleaf (*RMSE* = 16.090–19.437) and mixed stands (*RMSE* = 15.619–20.983), which could be attributable the high standard deviation (Table 2). When we compared the methods, the RK method gave more accurate results than the MLR method in both reflectance and vegetation indices values. The R^2 values of MLR and RK methods were 0.66 and 0.88 by using vegetation indices for coniferous stands. By performing the RK method, the model explanatory value increased by 8% using reflectance data in broadleaf stands and 16% by using vegetation indices in mixed stands. It was also seen that the RK method significantly improved the model accuracy. The variance of the residuals was decreased, and more accurate estimations were made with the effect of kriging (Benitez et al. 2016; Bolat et al. 2020).

Tsui et al. (2013) used the RK method based on airborne LIDAR and space-borne radar data to estimate AGB in managed forest area located on Vancouver Island, British Columbia, Canada. Correlation coefficients for 500, 1000, and 2000 m transects were obtained 0.68, 0.62, and 0.51, respectively. Li et al. (2015) used airborne LIDAR and SPOT 6 satellite data and estimated the AGB with MLR (R^2 = 0.48) and RK methods (R^2 = 0.66) in the northeast China. Li et al. (2020) predicted the AGB for coniferous, broadleaf, and mixed forests using MLR and RK methods in a subtropical monsoon humid climate zone in China. The R^2 values for the MLR method were 0.50, 0.52, and 0.43 for coniferous, broadleaf, and mixed forests, respectively. When the RK method was applied, these values were obtained as 0.86, 0.90, and 0.83, respectively. They increased the model explanatory power by 36–40% with the use of the RK method. The high increase in model accuracy compared to our study may be due to the greater diversity in the explanatory variables added to the model. Especially the use of texture datasets greatly contributes to the model explanatory in modeling studies with remote sensing data (Chrysafis et al. 2019; Bulut 2021).

As a combined method, the random forest-kriging (RFK) method was also used in AGB estimation. Chen et al. (2019a, b) estimated the AGB using random forest (RF) and RFK methods with ALOS-2, Sentinel-1,

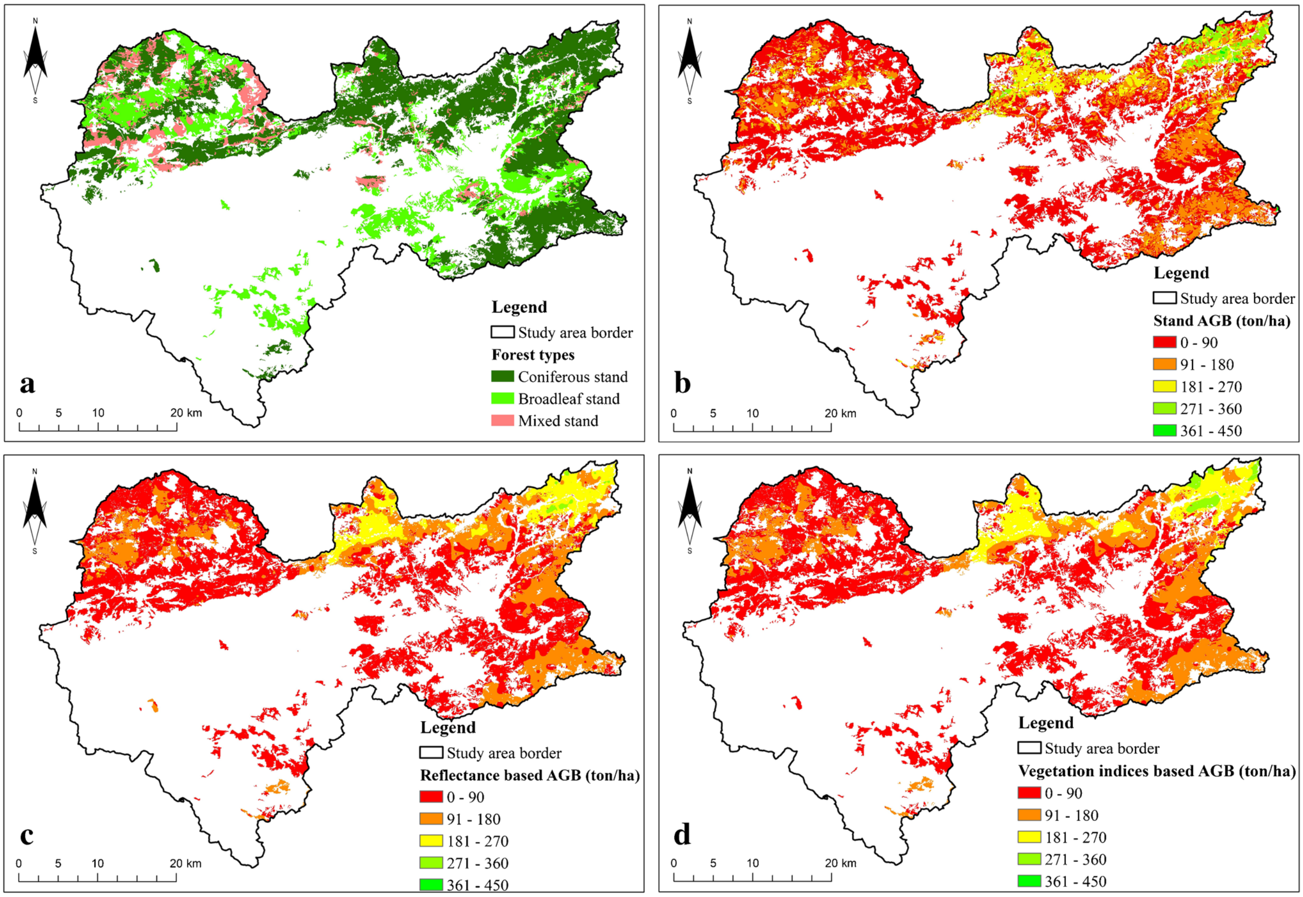

Fig. 4 Forest type map (**a**), reference surface map of AGB (**b**), predictions from the RK method based on **c** reflectance and **d** vegetation indices data

Sentinel-2, and topographical variables in eastern mountainous region of Jilin Province in northeast China. The R^2 and *RMSE* values were 0.985–30.24 (mg/ha) for RF method, and 0.990–28.15 (mg/ha) for RFK method. Su et al. (2020) modeled the AGB with RF and RFK methods using the digital elevation data and remotely sensed data such as ALOS/PALSAR and Landsat 5 TM for the years of 1992, 2002, and 2010 in Chinese subtropical forests. The highest accuracy improvement was obtained for 1992. The R^2 values were 0.41 and 0.81 for RF and RFK methods, respectively. In our study, coniferous stands have the highest SCI and lowest nugget effect, and the degree of accuracy improvement was higher in these stands. Su et al. (2020) found that the RF-based residuals had strong spatial autocorrelation in the data of 1992, and the highest increase in success was obtained in this year. For successful interpolations, especially in geostatistical methods, it was expected that the positional dependence was high, and the nugget effect was low. The low spatial autocorrelation limited the success of the estimation (Su et al. 2020; Li et al. 2020).

The fact that the areas with high AGB values in the reference map are low in the RK method is due to the combination of the kriging method. The method tends to overestimate low values and underestimate high values. This helps increase success by reducing the variance of error. In this study, high values are reduced by underestimating. Therefore, the stands with high AGB were determined lower in the RK method (Bolat et al. 2020).

However, the prediction of AGB in this study involves a shortcoming is that we used single-dated satellite imagery. As in our study, previous studies (Labrecque et al. 2006; Powell et al. 2010; Gasparri et al. 2010) have extensively used a single-date satellite image taken during the peak growing season to estimate AGB by developing empirical models. Satellite images obtained from different seasons give different texture measurements with changes in vegetation structure, soil background and sun angles, etc. (Culbert et al. 2009). The temporal information of satellite images can reduce the saturation problem, especially in estimating AGB in large areas (Zhu and Liu 2015; Gwenzi et al. 2017; Li et al. 2019). To capture cloud-free seasonal fluctuations of the vegetation, a high temporal resolution is required (Naik et al. 2021). As a result, it is critical to use seasonal time-series obtained from satellite images in order to reduce the saturation problem and improve the model's success in studies conducted in large areas with different vegetation structure. According to some studies in the literature, using seasonal time-series generated from different satellite images increased the success rates of predicted stand features (Wallner et al. 2015). According to Dymond et al. (2002), using seasonal time-series data to monitor forest parameters has the potential to increase accuracy. In a study conducted by Zhu and Liu (2015), it was stated that the saturation problem decreased, and the model success increased with the use of NDVI seasonal time-series data. Also, the author expressed that the phenological data provided in the time-series could help increase AGB estimation accuracy. Naik et al. (2021) stated that the AGB models based on multitemporal data were more effective in predicting than the single-time models, and spatial resolution is less important than spectral and temporal information for the prediction of AGB. Despite the forest ecosystem's heterogeneity and complexity, seasonal multi-temporal multispectral data outperformed single-dated image (Sullivan et al. 2018). As a result of, comparing the studies with optical images at a single time and seasonal multi-temporal data, we can say that the use of seasonal multi-time satellite data in the modeling of the AGB increases the model success.

Conclusion

Independent variables to model AGB were reflectance and vegetation indices data. The optimal data sets as explanatory variables were chosen using MLR method (Tables, 3, 4). The ordinary kriging method was used to create spatial distribution pattern of the residual AGB. Finally, MLR predictions and kriging residuals were combined, and produced RK estimations and maps. The results indicate the following: (1) the most appropriate reflectance and vegetation indices based on Sentinel-2 satellite image to prediction broadleaf stand AGB were B8 and PSSR in study area. (2) The AGB models of the MLR method were considered insufficient in terms of usability. (3) The RK method helped to minimize the residual variance of the predictions and to obtain more accurate estimations. (4) It was seen that combined method improved the model accuracy and gave the better results than pure method. (5) Neither exponential nor spherical model could fit the regression residuals well in semivariogram analysis due to the weak spatial dependency for broadleaf and mixed stands. (6) Although the RK model performances were a good level, it was inadequate in estimating the maximum AGB values. It would be helpful to estimate the AGB in different regions to clarify these results more consistently. Also, applying various remote sensing data and combinations of kriging and different statistical methods will help to overcome the problems in estimating AGB. Furthermore, single time based on multispectral data are insufficient for effectively modeling AGB in large forest areas, and greater modeling accuracy required multitemporal data. As a result, more studies into to the capabilities and limitations of seasonal Sentinel-2 time-series for AGB prediction are needed.

Acknowledgements We would like to thank to Turkish General Directorate of Forestry for providing data.

Declarations

Conflict of interest The authors declare no competing interests.

References

Abbas S, Wong MS, Wu J, Shahzad N, Irteza SM (2020) Approaches of satellite remote sensing for the assessment of above-ground biomass across tropical forests: pan-tropical to national scales. Remote Sens 12:3351. https://doi.org/10.3390/rs12203351

Ali G, Abbas S (2013) Exploring CO2 sources and sinks nexus through integrated approach: insight from Pakistan. J Environ Informatics 1:112–122. https://doi.org/10.3808/jei.201300250

Ali G, Nitivattananon V, Mehmood H, Sabir M, Sheikh S-R, Abbas S (2012) A synthesis approach to investigate and validate carbon sources and sinks of a mega city of developing country. Environ Dev 4:54–72. https://doi.org/10.1016/j.envdev.2012.09.001

Ali G, Abbas S, Pan Y, Chen Z, Hussain J, Sajjad M, Ashraf A (2019) Urban environment dynamics and low carbon society: multi-criteria decision analysis modeling for policy makers. Sustain Cities Soc 51:101763. https://doi.org/10.1016/j.scs.2019.101763

Anonymous (2018) Ilgaz Forest Enterprise, forest management plan, Turkish General Directorate of Forestry, Ankara. https://www.ogm.gov.tr

Behera SK, Shukla AK (2015) Spatial distribution of surface soil acidity, electrical conductivity, soil organic carbon content and exchangeable potassium, calcium and magnesium in some cropped acid soils of India. Land Degrad Dev 26(1):71–79

Benitez FL, Anderson LO, Formaggio AR (2016) Evaluation of geostatistical techniques to estimate the spatial distribution of aboveground biomass in the Amazon rainforest using high-resolution remote sensing data. Acta Amazon 46:151–160

Bhat MY, Arfat AS, Shambhu S (2021) Exploring environment-energy-growth nexus in OECD countries: a nonparametric approach. Biomass Convers Biorefinery. https://doi.org/10.1007/s13399-021-01835-w

Bolat F, Bulut S, Günlü A, Ercanlı İ, Şenyurt M (2020) Regression kriging to improve basal area and growing stock volume estimation based on remotely sensed data, terrain indices and forest inventory of black pine forests. New Zealand J For Sci. https://doi.org/10.33494/nzjfs502020x49x

Bulut S (2021) Ankara Orman Bölge Müdürlüğü saf karaçam meşcerelerinde net birincil üretim ve yaprak alan indeksinin uzaktan algilama teknikleri ile modellenmesi. Modeling net primary productivity and leaf area index with remote sensing techniques in pure crimean pine stands in Ankara Regional Directorate of Forestry, Çankırı Karatekin University, Graduate School of Natural and Applied Sciences, Phd thesis, p 161

Cambardella C, Moorman T, Parkin T, Karlen D, Novak J, Turco R, Konopka A (1994) Field-scale variability of soil properties in central Iowa soils. Soil Sci Soc Am J 58(5):1501–1511

Castillo-Santiago MÁ, Ghilardi A, Oyama K, Hernández-Stefanoni JL, Torres I, Flamenco-Sandoval A, Mas JF (2013) Estimating the spatial distribution of woody biomass suitable for charcoal making from remote sensing and geostatistics in central Mexico. Energy Sustain Dev 17(2):177–188

Chen L, Wang Y, Ren C, Zhang B, Wang Z (2019) Optimal combination of predictors and algorithms for forest above-ground biomass mapping from Sentinel and SRTM data. Remote Sensing 11(4):414

Chen L, Wang Y, Ren C, Zhang B, Wang Z (2019) Assessment of multi-wavelength SAR and multispectral instrument data for forest aboveground biomass mapping using random forest kriging. For Ecol Manage 447:12–25

Chen L, Ren C, Zhang B, Wang Z (2020) Multi-sensor prediction of stand volume by a hybrid model of support vector machine for regression kriging. Forests 11(3):296

Chrysafis I, Mallinis G, Tsakiri M, Patias P (2019) Evaluation of single-date and multi-seasonal spatial and spectral information of Sentinel-2 imagery to assess growing stock volume of a Mediterranean forest. Int J Appl Earth Obs Geoinf 77:1–14

Clerici N, Rubiano K, Abd-Elrahman A, Posada Hoestettler JM, Escobedo FJ (2016) Estimating aboveground biomass and carbon stocks in periurban Andean secondary forests using very high resolution imagery. J Forest 7(138):17. https://doi.org/10.3390/f7070138

Cressie NAC (1993) Statistics for Spatial Data. John Wiley & Sons, New York, USA, p 416

Culbert PD, Pidgeon AM, St. Louis V, Radeloff VC, Bash D (2009) The impact of phenological variation on texture measures of remotely sensed imagery. IEEE J Sel Top Appl Earth Obs Remote Sens 2, 299–309

Deb D, Singh JP, Deb S, Datta D, Ghosh A, Chaurasia RS (2017) An alternative approach for estimating above ground biomass using Resourcesat-2 satellite data and artificial neural network in Bundelkhand region of India. Environ Monit Assess 189(11) 576, 12p. https://doi.org/10.1007/s10661-017-6307-6

Dymond CC, Mladenoff DJ, Radeloff VC (2002) Phenological differences in Tasseled Cap indices improve deciduous forest classification. Remote Sens Environ 80:460–472

Englhart S, Keuck V, Siegert F (2011) Aboveground biomass retrieval in tropical forests-the potential of combined X- and L-band SAR data use. Reote Sens Environ 115:1260–1271

Gasparri NI, Parmuchi MG, Bono J, Karszenbaum H, Montenegro CL (2010) Assessing multi-temporal Landsat 7 ETM+ images for estimating above-ground biomass in subtropical dry forests of Argentina. J Arid Environ 74:1262–1270

Goetz S, Baccini A, Laporte N, Johns T, Walker W, Kellndorfer J, Houghton R, Sun M (2009) Mapping and monitoring carbon stocks with satellite observa-tions: a comparison review. Carbon Balance Manage 4(2):1–7

Goovaerts P (2000) Geostatistical approaches for incorporating elevation into the spatial interpolation of rainfall. J Hydrol 228(1–2):113–129

Günlü A, Ercanli I, Başkent EZ, Çakır G (2014) Estimating aboveground biomass using Landsat TM imagery: a case study of Anatolian Crimean pine forests in Turkey. Ann for Res 57(2):289–298

Gwenzi D, Helmer E, Zhu X, Lefsky M, Marcano-Vega H (2017) Predictions of tropical forest biomass and biomass growth based on stand height or canopy area are improved by Landsat-scale phenology across Puerto Rico and the U.S. Virgin Islands. Remote Sens 9:123

Hall RJ, Skakun RS, Arsenault EJ (2006) Modeling forest stand structure attributes using Landsat ETM+ data: application to mapping of aboveground biomass and stand volume. For Ecol Manage 225:378–390

Hengl T, Heuvelink GBM, Rossiter DG (2007) About regression-kriging: from equations to case studies. Comput Geosci 33(10):1301–1315

Hu H, Wang GG (2008) Changes in forest biomass carbon storage in the South Carolina Piedmont between 1936 and 2005. For Ecol Manage 255:1400–1408

Ji L, Wylieb BK, Nossovc DR, Petersona B, Waldropd MP, McFarlandd JW, Roverb J, Hollingsworth TN (2012) Estimating aboveground biomass in interior Alaska with Landsat data and field measurements. Int J Appl Earth Obs Geoinf 18:451–461

Kumar K, Nagai M, Witayangkurn A, Kritiyutanant K, Nakamura S (2016) Above ground biomass assessment from combined optical and SAR remote sensing data in Surat Thani Province, Thailand. J Geogr Inf Syst 8, 506–516 http://www.scirp.org/journal/jgis.

Labrecque S, Fournier RA, Luther JE, Piercey D (2006) A comparison of four methods to map biomass from Landsat-TM and inventory data in western Newfoundland. For Ecol Manage 226:129–144

Laurin GV, Puletti N, Hawthorne W, Liesenberg V, Corona P, Papale D, Chen Q (2016) Valentini, R. Discrimination of tropical forest types, dominant species, and mapping of functional guilds by hyperspectral and simulated multispectral Sentinel-2 data. Remote Sens Environ 176:163–176

Li W, Niu Z, Liang X, Li Z, Huang N, Gao S, Wang C, Muhammad S (2015) Geostatistical modeling using LiDAR-derived prior knowledge with SPOT-6 data to estimate temperate forest canopy cover and above-ground biomass via stratified random sampling. Int J Appl Earth Obs Geoinf 41:88–98

Li G, Xie Z, Jiang X, Lu D, Chen E (2019) Integration of ZiYuan-3 multispectral and stereo data for modeling aboveground biomass of larch plantations in North China. Remote Sens 11:2328

Li Y, Li M, Liu Z, Li C (2020) Combining Kriging interpolation to improve the accuracy of forest aboveground biomass estimation using remote sensing data. IEEE Access 8:128124–128139

Lu D (2006) The potential and challenge of remote sensing-based biomass estimation. Int J Remote Sens 27:1297–1328

Motlagh MG, Kafaky SB, Mataji A, Akhavan R (2018) Estimating and mapping forest biomass using regression models and Spot-6 images (case study: Hyrcanian forests of north of Iran). Environ Monit Assess 190(6):1–14

Mura M, Bottalico F, Giannetti F, Bertani R, Giannini R, Mancini M, Orlandini S, Travaglini D, Chirici G (2018) Exploiting the capabilities of the Sentinel-2 multi spectral instrument for predicting growing stock volume in forest ecosystems. Int J Appl Earth Obs 66:126–134

Naik P, Dalponte M, Bruzzone L (2021) Prediction of forest aboveground biomass using multitemporal multispectral remote sensing data. Remote Sens 13:1282

Navarro JA, Algeet N, Fernández-Landa A, Esteban J, Rodríguez-Noriega P (2019) Guillén-Climent ML (2019) Integration of UAV, Sentinel-1, and Sentinel-2 data for mangrove plantation aboveground biomass monitoring in Senegal. Remote Sens 11:77. https://doi.org/10.3390/rs11010077

Odeh IOA, McBratney AB, Chittleborough DJ (1994) Spatial prediction of soil properties from landform attributes derived from a digital elevation model. Geoderma 63:197–214

Odeh IOA, McBratney AB, Chittleborough DJ (1995) Further results on prediction of soil properties from terrain attributes: heterotopic cokriging and regression kriging. Geoderma 67(3–4):215–226

Pandit S, Tsuyuki S, Dube T (2018) Estimating above-ground biomass in sub-tropical buffer zone community forests, Nepal, using Sentinel 2 data. Remote Sens 10:601. https://doi.org/10.3390/rs10040601

Powell SL, Cohen WB, Healey SP, Kennedy RE, Moisen GG, Pierce KB, Ohmann JL (2010) Quantification of live aboveground forest biomass dynamics with Landsat time-series and field inventory data: a comparison of empirical modeling approaches. Remote Sens Environ 114:1053–1068

Romero LS, Marcello J, Vilaplana V (2020) Super-resolution of Sentinel-2 imagery using generative adversarial networks. Remote Sens 12:2424. https://doi.org/10.3390/rs12152424

Ronoud G, Fatehi P, Darvishsefat AA, Tomppo E, Praks J, Schaepman ME (2021) Multi-sensor aboveground biomass estimation in the broadleaved Hyrcanian forest of Iran. Can J Remote Sens 47(6):818–834

Schroeder P, Brown S, Mo J, Birdsey R, Cieszewski C (1997) Biomass estimation for temperate broadleaf forests of the United States using inventory data. For Sci 43:424–434

Sibanda M, Mutanga O, Rouget M (2015) Examining the potential of Sentinel-2 MSI spectral resolution in quantifying above ground biomass across different fertilizer treatments. ISPRS J Photogramm Remote Sens 110:55–65

Su H, Shen W, Wang J, Ali A, Li M (2020) Machine learning and geostatistical approaches for estimating aboveground biomass in Chinese subtropical forests. For Ecosyst 7(1):1–20

Sullivan MJP, Lewis SL, Hubau W, Qie L, Baker TR, Banin LF, Chave J, Cuni-Sanchez A, Feldpausch TR, LopezGonzalez G et al (2018) Field methods for sampling tree height for tropical forest biomass estimation. Methods Ecol Evol 9:1179–1189

Teobaldelli M, Somogyi Z, Migliavacca M, Usoltsev VA (2009) Generalized functions of biomass expansion factors for conifers and broadleaved by stand age, growing stock and site index. For Ecol Manage 257:1004–1013

Tian X, Su Z, Chen E, Li Z, van der Tol C, Guo J, He Q (2012) Estimation of forest above-ground biomass using multi-parameter remote sensing data over a cold and arid area. Int J Appl Earth Obs Geoinf 14:160–168

Tolunay D (2011) Total carbon stocks and carbon accumulation in living tree biomass in forest ecosystems of Turkey. Turkish J Agric for 35:265–279

Tsui OW, Coops NC, Wulder MA, Marshall PL (2013) Integrating airborne LiDAR and space-borne radar via multivariate kriging to estimate above-ground biomass. Remote Sens Environ 139:340–352

Viana H, Aranha J, Lopes D, Cohen W (2012) Estimation of crown biomass ofPinus pinaster stands and shrubland above-ground biomass using inventory data, remotely sensed imagery and spatial prediction models. Ecol Model 226:22–35

Wallner A, Elatawneh A, Schneider T, Knoke T (2015) Estimation of forest structural information using RapidEye satellite data. Forestry 88:96–107

Wang X, Jiao H (2020) Spatial scaling of forest aboveground biomass using multi-source remote sensing data. IEEE Access 8:178870–178885

Zheng D, Rademacher J, Chen J, Crow T, Bresee M, Le Moine J, Ryu S (2004) Estimating aboveground biomass using Landsat 7 ETM+ data across a Biomass estimation managed landscape in northern Wisconsin, USA. Remote Sens Environ 93:402–411

Zhu X, Liu D (2015) Improving forest aboveground biomass estimation using seasonal Landsat NDVI time-series. ISPRS J Photogramm Remote Sens 102:222–231